Dynamic Model Based Friction Compensation on the Furuta Pendulum

Gäfvert, Magnus

1999

Dynamic Model Based Friction Compensation on the Furuta Pendulum

Magnus Gäfvert

Dept. of Automatic Control
Lund Institute of Technology
PB 118, S-221 00 LUND, Sweden
magnus@control.lth.se

Abstract The Furuta pendulum is used to evaluate a friction compensator based on the dynamic LuGre friction model. The effect of friction compensation is very well illustrated by reduction of limit cycles when stabilising the pendulum. The observer based LuGre friction compensator is compared with classical Coulomb and Stiction compensator schemes. Existing analysis of the LuGre observer is extended to observer based friction compensation in general linear state feedback control of linear time invariant systems where friction enters the system at the input. In particular this observer based friction compensation is applicable on the pendulum. The performance of the LuGre compensator was found to be similar to that of the Stiction compensator. Important differences is the smooth control signal obtained from the LuGre observer, and that it uses less prior information.

1. Introduction

Friction is present in all mechanical systems. It poses difficult challenges to control engineers. In recent years several works have addressed the problem of friction modelling and compensation using increasingly sophisticated methods [8]. The motivation behind this interest is the growing number of applications with precision positioning in mechanical systems. Much effort has been imposed on theoretical work and simulations [3, 6, 9], while other work focus on practice and experiments [2, 5, 11]. There are several methods and results that are well understood theoretically, that have yet to be tried in real applications. The availability of fast DSPs and precision sensors makes it possible to implement advanced algorithms with reasonable effort. The objective of this paper is to exploit the properties of one such algorithm in practice. The LuGre model [3] will be used for model based friction compensation in stabilisation of a Furuta pendulum. The results are compared with those of classical model based friction compensation. The paper is a natural extension to the simulation works in [6], although the controlled system is of higher complexity in this work. The reason for using the Furuta pendulum as an example application is that friction greatly deteriorates control performance. The friction nonlinearity result in large limit cycles when using linear state feedback stabilisation. With efficient friction compensation the limit cycles can be eliminated.

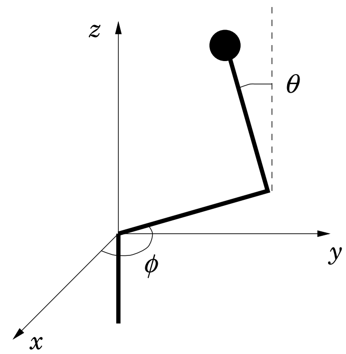

Figure 1 The Furuta pendulum.

2. The Furuta Pendulum

The Furuta pendulum [4] consists of two connected inertial bodies; An actuated rotating center pillar rigidly connected to a horisontal arm, and a pendulum arm connected to the horisontal arm by a 1-DOF joint, see Figure 1. The arm position is denoted by ϕ, the pendulum position by θ, and their corresponding time derivatives by $\dot{\phi}$ and $\dot{\theta}$. The pendulum is driven by a torque input u on the horisontal arm. The ϕ joint exhibits significant friction. Let F denote the friction torque. The friction on the pendulum joint is assumed to be negligable. Let $x \triangleq \left(\phi, \dot{\phi}, \theta, \dot{\theta}\right)^T$. The linearized dynamics of the pendulum at the unstable upright position are

$$\frac{dx}{dt} = Ax + B(u - F) \tag{1}$$

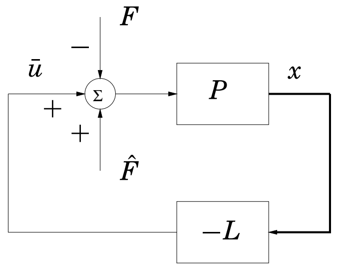

Figure 2 State feedback control with model based friction compensation.

with

$$A = \begin{pmatrix} 0 & 1 & 0 & 0 \\ 0 & 0 & a_{23} & 0 \\ 0 & 0 & 0 & 1 \\ 0 & 0 & a_{43} & 0 \end{pmatrix}, \qquad B = \begin{pmatrix} 0 & 0 \\ b_{21} & \\ 0 & 0 \\ b_{41} & \end{pmatrix} \tag{2}$$

The eigenvalues of A are $\{0, 0, \pm\sqrt{a_{43}}\}$.

3. Control Strategy

The control objective is to stabilise the pendulum around the unstable equilibrium at the upright position. A model based friction compensation scheme is used to reduce the effect of friction, see Figure 2. A friction model is used to obtain a friction estimate $\hat{F}$, which is added to the control input

$$u = \hat{F} + \bar{u} \tag{3}$$

Since the control input and the friction enter the system at the same place, the real friction torque is thus cancelled if $\hat{F} - F = 0$. The remaining process is linear, and a linear state feedback controller

$$\bar{u} = -Lx \tag{4}$$

is designed for (2) to stabilise the pendulum. The feedback gain L is chosen such that the closed loop system has the characteristic equation

$$(s^2 + 2\zeta_1\omega_1 s + \omega_1^2)(s^2 + 2\zeta_2\omega_2 s + \omega_2^2) = 0 \tag{5}$$

All states of (2) can be measured. The design is made in continuous time, and then implemented in sampled digital form with fast sampling rate.

4. Friction Models

4.1 Coulomb Friction

The most commonly used friction model is the Coulomb model

$$F = F_C \operatorname{sgn}(\dot{\phi}) \tag{6}$$

A friction estimate for compensation is obtained from this model as

$$\hat{F} = \begin{cases} F_C \operatorname{sgn}(\dot{\phi}) & \text{if } |\dot{\phi}| > \delta v, \\ F_C v/\delta v & \text{if } |\dot{\phi}| \le \delta v \end{cases} \tag{7}$$

The friction estimate is nonsmooth, which can be a problem is certain applications. The constant δv is used to avoid the discontinuity at $\dot{\phi} = 0$. Although very simple this model captures the essential behavior of friction, and has shown to be useful in many applications.

4.2 Coulomb Friction with Stiction

The next level of sophistication is to introduce stiction in the friction model. Stiction is the phenomenon that initiating a motion requires a larger force than retaining it. The simplest memoryless friction model with stiction is

$$F = \begin{cases} F_C \operatorname{sgn}(\dot{\phi}) & \text{if } \dot{\phi} \ne 0, \\ \bar{F} & \text{if } \dot{\phi} = 0 \text{ and } |\bar{F}| < F_s, \\ F_s \operatorname{sgn}(\bar{F}) & \text{otherwise.} \end{cases} \tag{8}$$

with $\bar{F}$ being the resultant forces acting at the friction joint. In the case of the pendulum $\bar{F} = a_{23}\theta + b_{21}u$. Note that friction is modelled as a function of $\dot{\phi}$ and $\bar{F}$. The commonly used notation to regard friction as a function of only the velocity is thus wrong in this case. An estimate for compensation is constructed as

$$\hat{F} = \begin{cases} F_s \operatorname{sgn}(\bar{F}) & \text{if } \dot{\phi} = 0, \\ F_C \operatorname{sgn}(\dot{\phi}) & \text{if } \dot{\phi} \ne 0 \end{cases} \tag{9}$$

Note that the compensation term is a function of both $\dot{\phi}$ and $\bar{F}$. This compensation term efficiently eliminates the friction, though the control signal becomes discontinuous and chattering at velocities close to zero. Therefore this model is not commonly used in applications. It is reasonable to use the model for comparison with other compensation strategies though.

4.3 LuGre Friction

One motivation behind the LuGre model is to offer a regularised Coulomb model with stiction. The model captures several friction characteristics, such as increased friction torque at lower velocities, see [6]. It is a first order dynamic model. The most commonly used form is

$$\begin{aligned} \frac{dz}{dt} &= v - \sigma_0 \frac{|v|}{g(v)} z \\ g(v) &= \alpha_0 + \alpha_1 e^{-(v/v_s)^2} \\ F &= \sigma_0 z + \sigma_1 \frac{dz}{dt} \end{aligned} \tag{10}$$

with α_0, α_1, v_s, σ_0 and σ_1 positive parameters. In the present system $v \equiv \dot{\phi}$. Since the state z cannot be measured, it is necessary to use an observer to get an estimate of the friction based on the LuGre model.

4.4 LuGre Friction Observers

For Coulomb friction and stiction the friction force can be determined directly from measurable quantities. Since the LuGre model is dynamic it is necessary to use an observer for the friction force.

Open Loop Observers Since the dynamics in the LuGre model is stable and fast the simplest solution is to use the open loop observer

$$\begin{aligned}\frac{d\hat{z}}{dt} &= v - \left(\varepsilon + \sigma_0 \frac{|v|}{g(v)}\right)\hat{z} \\ \hat{F} &= \sigma_0 \hat{z} + \sigma_1 \frac{d\hat{z}}{dt}\end{aligned} \tag{11}$$

where the regularization parameter ε has been introduced to avoid a potential problem at $v = 0$. This regularization parameter can be interpreted as a relaxation time constant for the deflected bristles when regarding the LuGre model as a bristle model, see [3].

Observers with Feedback A more complicated observer is obtained by introducing feedback from other signals in the system. The observer then becomes

$$\begin{aligned}\frac{d\hat{z}}{dt} &= v - \sigma_0 \frac{|v|}{g(v)}\hat{z} - ke \\ \hat{F} &= \sigma_0 \hat{z} + \sigma_1 \frac{d\hat{z}}{dt}\end{aligned} \tag{12}$$

where the observer feedback e is a signal related to the estimation error. In [3, 6, 7] the performance of friction compensation based on this observer in the control of a simple servo is studied. It is suggested to use the control error as observer feedback but many choices are possible. In the particular case of the Furuta pendulum this may lead to instability. In the remaining part of this section the observer based friction compensation in a general setup with linear state feedback control of a linear time invariant system is studied. Friction is assumed to enter the system at the input. The results are applicable to the Furuta pendulum.

Let the observer feedback term be chosen as $e \triangleq Kx$, where x is the measurable state of the system. Let $\tilde{F} \triangleq F - \hat{F}$ and $\tilde{z} \triangleq z - \hat{z}$. The error equation

$$\frac{d\tilde{z}}{dt} = -\sigma_0 \frac{|v|}{g(v)}\tilde{z} + kKx \tag{13}$$

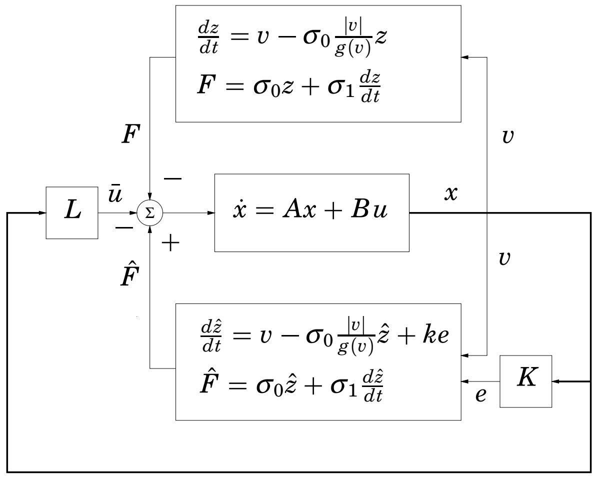

Figure 3 LuGre observer based friction compensation and linear state feedback.

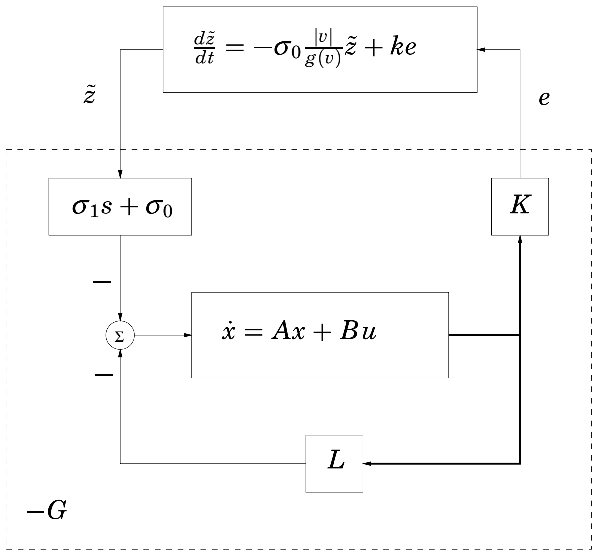

Figure 4 LuGre observer based friction compensation and linear state feedback as an interconnection of SPR and passive systems.

is obtained by subtracting (10) by (12). The closed loop system (1), (3), (4), (10) and (12) can be described with the block diagram in Figure 3.

Partitioning of the closed loop system into a linear and a nonlinear part yields the block diagram in Figure 4. It is seen that

$$e = -\frac{K(sI - A)^{-1}B(\sigma_1 s + \sigma_0)}{1 + L(sI - A)^{-1}B}\tilde{z} \triangleq -G\tilde{z} \tag{14}$$

Proposition 1: If G is stable with no poles on the imaginary axis and (A,B) is controllable then there always exist a K such that G is strictly positive real (SPR).

Proof: Since (A,B) is controllable it is possible to choose K such that G has relative degree zero, and to arbitrarily position all but one of the zeros of G. It is thus always possible to position the zeros strictly inside the left half-plane, such that they cancel all but one poles of G, or all but two poles if the poles are complex. If all poles but one are cancelled SPR follows trivially. In the other case it is straightforward to show that one can always position the remaining zero such that the phase of G lies strictly in the interval $(-\pi/2, \pi/2)$. □

Proposition 2: Consider the system (1), (3), (4), (10) and (12), with L chosen such that $A + BL$ is Hurwitz. If K is chosen such that G is SPR then the observer error $\tilde{F}$ and the states x will go to zero asymptotically, and the system is stable.

Proof: Regard first the decomposition (14). It is well known that (13) constitutes a passive map from e to $\tilde{z}$ [3, 6]. When G is SPR asymptotic stability follows directly from the passivity theorem. Thus $\tilde{F} \rightarrow 0$ asymptotically, and the state x of the remaining asymptotically stable LTI system $A + BL$ goes to zero asymptotically. From (10) it follows that $||F|| \leq \sigma_0||z|| + \sigma_1||v|| + \sigma_0\sigma_1/\alpha_0\, ||v||\, ||z||$. It is well known that z in (10) is bounded [3]. Since x, and therefore v, is bounded, F is bounded and the system is stable. □

Friction compensation for the Furuta pendulum based on the LuGre model is thus established by choosing K appropriately and adding the friction estimate given by (12) to the state feedback control input.

5. Experiments

5.1 The Setup

The experiments are carried out on the pendulum in Figure 5. The control algorithms are implemented with RealLink/32 [10], an extension to Simulink and Real-time Workshop for Matlab. RealLink/32 is a very convenient tool for rapid implementation of control algorithms. The tight Matlab integration makes it easy to use standard Matlab procedures for controller design and analysis of controller performance. The control algorithms are implemented as Simulink blocks, which are then translated to C-code. Finally an Windows NT executable is built. Reallink/32 provides a small real-time kernel that is used to run the executable. A standard Pentium PC with a 12 bit AD/DA-converter board is booted with the real-time kernel and then loaded with the controller program. The sampling rate is chosen to 1 ms.

The horisontal arm is actuated with a high gain current controlled DC motor. The actuator dynamics are negligable in the context of pendulum stabilisation.

Figure 5 The Furuta pendulum

The control input is normalised to the range -10 to 10 [V]. The pendulum is further equipped with an incremental decoder of 250 pulses per revolution for measuring the horisontal arm position ϕ. The horisontal arm velocity $\dot{\phi}$ is measured with a tachometer. The pendulum position θ is measured with a potentiometer. A resolution $3.8 \cdot 10^{-4}$ [rad] is achieved by using the 12 bits of the AD converter in the range $-\pi/4$ [rad] to $\pi/4$ [rad]. A low-pass filter is used to reduce the measurement noise. The filter is also used to obtain a velocity estimate for $\dot{\theta}$, since the derivative of the filtered position is available as an internal state in the filter implementation, see [11].

The coefficients of the linearized pendulum dynamics (2) are identified by means of least-squares estimation to be $a_{23} = -11, a_{43} = 33$, $b_{21} = 45$ and $b_{22} = -29$. The eigenfrequency of the linearized stable equilibrium is 5.7 [rad/s]. The identification procedure also gives a measure of the Coulomb friction $F_C = 0.21$, normalised to the control signal. The friction is significantly large.

The feedback gain L in (4) is chosen such that $\omega_1 = 7$ [rad/s], $\omega_2 = 5$ [rad/s] and $\zeta_1 = \zeta_2 = 0.7$ in (5).

5.2 No Friction Compensation

Stabilisation of the pendulum with the linear control law (4) without friction compensation is shown in Figure 6. The system exhibits large limit cycles due to the friction. Note that the horisontal arm gets stuck as

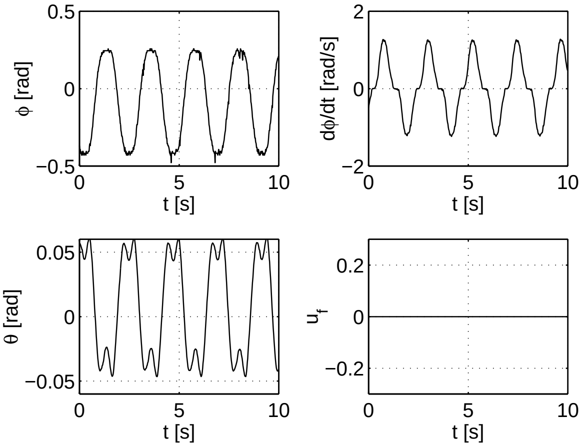

Figure 6 Experimental results without friction compensation. The plots are: Arm position ϕ (upper left), arm velocity $\dot{\phi}$ (upper right), pendulum position θ (lower left), and the friction compensating part of the control signal, i.e. the estimated friction $\hat{F}$ (lower right).

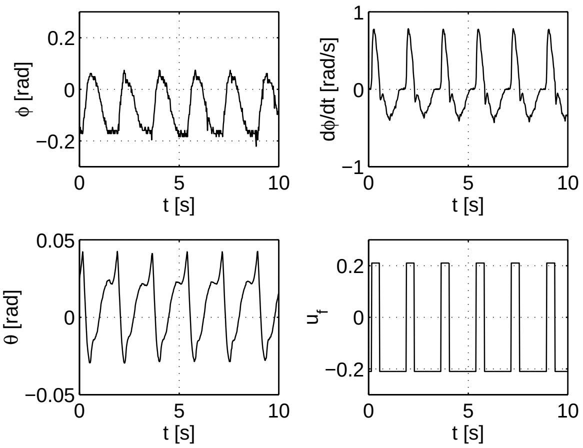

Figure 7 Experimental results with Couolomb friction compensation. The plots are: Arm position ϕ (upper left), arm velocity $\dot{\phi}$ (upper right), pendulum position θ (lower left), and the friction compensating part of the control signal, i.e. the estimated friction $\hat{F}$ (lower right).

velocity changes sign. This is characteristic for friction induced limit cycles. The asymmetry in the signals is due to asymmetric friction characteristics.

5.3 Coulomb Friction Compensation

With Coulomb compensation (7) with $F_C = 0.21$ the size of the limit cycles are considerably reduced, see Figure 7. The standard deviations of ϕ, θ and the linear control signal u are given in Table 1.

5.4 Coulomb + Stiction Friction Compensation

With Coulomb and stiction compensation (9) with $F_C = 0.21$ and $F_s = 0.25$ added to the controller the performance is further improved. The effect of friction

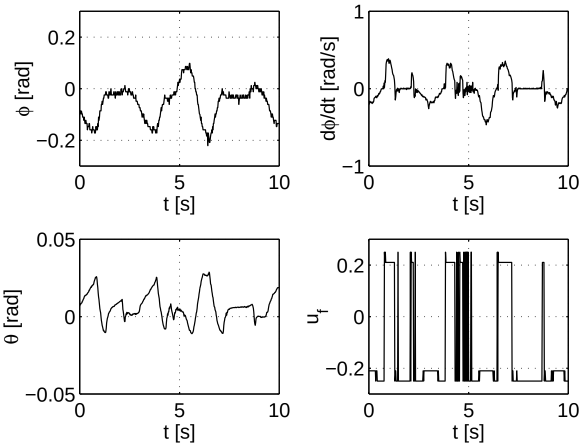

Figure 8 Experimental results with stiction friction compensation. The plots are: Arm position ϕ (upper left), arm velocity $\dot{\phi}$ (upper right), pendulum position θ (lower left), and the friction compensating part of the control signal, i.e. the estimated friction $\hat{F}$ (lower right).

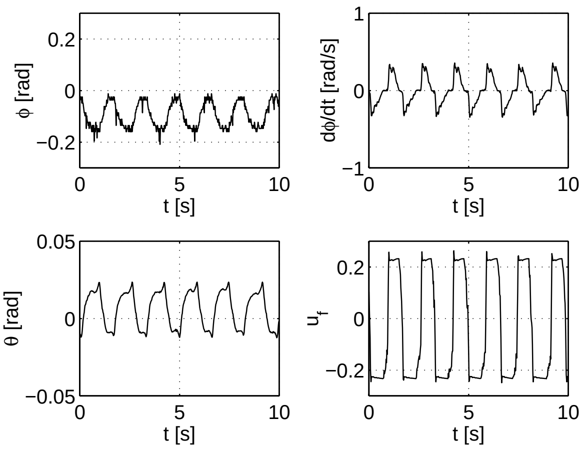

Figure 9 Experimental results with LuGre friction compensation. The plots are: Arm position ϕ (upper left), arm velocity $\dot{\phi}$ (upper right), pendulum position θ (lower left), and the friction compensating part of the control signal, i.e. the estimated friction $\hat{F}$ (lower right).

can be practically eliminated if F_C and F_s are chosen correctly. Time variations and asymmetry in the friction characteristics makes this difficult, and Figure 8 shows typical performance. (Note the different scaling in the figures.) The friction compensation signal is very nonsmooth and chattering. Mechanical vibrations that are excited by the chattering also helps in reducing the effects of friction. Introduction of dither is a well known strategy for handling friction.

5.5 LuGre Friction Compensation

With LuGre compensation (11) the results in Figure 9 are obtained. The parameters are $\alpha_0 = 0.21$, $\alpha_1 = 0.022$, $\sigma_0 = 80$, $\sigma_1 = 1.5$ and $\varepsilon = 0$. Suitable values of the parameters α_0 and α_1 are indicated by F_C and F_s above. The other parameters were found by manually tuning the compensator. The control performance is equal to that of the previous case. The great advantage is that the same performance can be achieved with a smooth control signal.

5.6 Summary

A summary of the performance of the compensation schemes is given i Table 1. The Coulomb + Stiction and LuGre compensation schemes are very good at reducing the effects of friction. It should be noted that the Stiction scheme uses more information than the LuGre model as it needs the linear control signal. Practically this is usually not a problem since this signal normally is available. However, it is noteworthy that the LuGre scheme can give the same performance with less information. The main difficulty with friction compensation of the type in this paper is that the friction characteristics vary with time. This motivates the use of adaptive schemes, [2, 9]. The motor used in the pendulum has brushes. Therefore the friction characteristics are asymmetric. This motivates the use of asymmetric compensation, see see [1]. It is straightforward to modify the compensation schemes in this paper to the asymmetric case.

Friction compensation	σ_ϕ	$\sigma_{\dot\phi}$	u
None	0.26	0.040	0.22
Coulomb	0.086	0.020	0.11
Coulomb + Stiction	0.066	0.0092	0.065
LuGre	0.048	0.012	0.062

Table 1 Standard deviations on arm position ϕ, arm velocity $\dot\phi$, and linear control signal $\bar{u}$ for different friction compensation strategies during stabilisation of the Furuta pendulum.

6. Conclusions

The Furuta pendulum was used to evaluate friction compensators. The effect of friction compensation was very well illustrated by reduction of limit cycles when stabilising the pendulum. The observer based LuGre friction compensator was compared with classical Coulomb and Stiction compensator schemes. Existing analysis of the LuGre observer was extended to observer based friction compensation in general linear state feedback control of linear time invariant systems where friction enters the system at the input. It was shown how to construct the observer feedback in this case. In particular this observer based friction compensation is applicable on the pendulum. The performance of the LuGre compensator was found to be similar to that of the Stiction compensator. An important difference is the smooth friction estimate obtained from the LuGre observer.

7. References

[1] C. Canudas de Vit, Karl Johan Åström, and K. Braun. Adaptive friction compensation in DC-motor drives. *IEEE Trans. Robotics and Automation*, RA-3:681–685, 1987.

[2] Carlos Canudas de Wit and Pablo Lischinsky. Adaptive friction compensation with dynamic friction model. In *IFAC-WC*, 1996.

[3] Carlos Canudas de Wit, Henrik Olsson, Karl Johan Åström, and Pablo Lischinsky. A new model for control of systems with friction. *IEEE Transactions on Automatic Control*, 40(3), March 1995.

[4] K. Furuta, M. Yamakita, S. Kobayashi, and M. Nishimura. A new inverted pendulum apparatus for eduction. In *IFAC Symposium on Advances in Control Education, Boston*, pages 191–196, 1994.

[5] Pablo A. Lischinsky. *Compensation de frottement et commande en position d'un robot hydraulique industriel*. PhD thesis, Laboratiore d'Automatique de Grenoble - ENSIEG, France, May 1997.

[6] Henrik Olsson. *Control Systems with Friction*. PhD thesis, Lund Institute of Technology, University of Lund, 1996.

[7] Henrik Olsson and Karl-Johan Åström. Observer-based friction compensation. In *35th IEEE Conf. on Decision and Control*, pages 4345–5450, Kobe, Japan, 1996.

[8] Henrik Olsson, Karl Johan Åström, Carlos Canudas de Wit, Magnus Gäfvert, and Pablo Lischinsky. Friction models and friction compensation. *European Journal of Control*, 1998(4):176–195, 1998.

[9] Elena Panteley, Romeo Ortega, and Magnus Gäfvert. An adaptive friction compensator for global tracking in robot manipulators. In *Proc. SYROCO'97, 5th IFAC Symposium on Robot Control*, Nantes, 1997.

[10] RealTech AG, Switzerland. *RealLink/32 — User's Manual*, 1998.

[11] Joakim Svensson. Effects of friction on the Furuta pendulum. Technical report, January 1998.